

Identification of a putative binding site for 5-alkyl-benzothiadiazides in the AMPA receptor dimer interface

Kasper Harpsøe^a, Thomas Varming^b, Alex Haahr Gouliaev^{b,1},
Dan Peters^b, Tommy Liljefors^{a,*}

^aDepartment of Medicinal Chemistry, The Danish University of Pharmaceutical Sciences, Universitetsparken 2, DK-2100 Copenhagen, Denmark

^bDepartment of Medicinal Chemistry, NeuroSearch A/S, Pederstrupvej 93, DK-2750 Ballerup, Denmark

Received 29 May 2006; received in revised form 5 July 2006; accepted 5 July 2006

Available online 11 July 2006

Abstract

Crystal structures of three different allosteric modulators co-crystallized with the iGluR2 ligand-binding domain are currently available. The modulators, cyclothiazide, aniracetam and CX614, bind at overlapping binding sites in the dimer interface between two iGluR2 subunits. However, pharmacological data indicate that there are one or more additional binding sites for this class of compounds. Based on differences in structure–activity relationship data we show that 5-alkyl-benzothiadiazide (5ABTD) modulators and a series of close analogs of cyclothiazide, despite having a common core structure, do not have the same binding site. In the present work, a new potential binding site for allosteric modulators has been identified in the dimer interface of the iGluR2 ligand-binding domain. By comparing different iGluR2 crystal structures including different co-crystallized agonists, this cavity is shown to be a structurally conserved part of the dimer interface. The cavity is characterized with respect to shape and potential favorable interactions with ligands and docking is used to find a reasonable binding mode for the core structure of the 5ABTDs. The extensive structure–activity data available for this series of compounds are in agreement with the proposed binding mode, supporting the conclusion that the identified cavity most likely is the binding site for the 5ABTDs.

© 2006 Elsevier Inc. All rights reserved.

Keywords: AMPA receptor; Allosteric modulator; Docking; Molecular interaction fields; Structure–activity analysis

1. Introduction

The α -amino-3-hydroxy-5-methyl-4-isoxazolepropionic acid (AMPA) receptors are a subclass of the ionotropic glutamate receptors (iGluRs), which are widespread in the mammalian nervous system. The AMPA receptors which contain the subunits iGluR1–4 are involved in learning and memory and play a role in several neurodegenerative diseases. These receptors are ligand gated ion channels and each subunit consists of an extracellular part containing the ligand-binding domain (LBD) and a transmembrane part constituting the ion channel [1]. Extensive knowledge have been obtained about the regulation of the AMPA receptors through crystal structures of a construct of the isolated

LBD of iGluR2 [2]. As illustrated in Fig. 1, the LBD consists of two domains. When an agonist is bound, domain 2 closes up towards domain 1 moving the residues connected to the transmembrane part and causes the channel to open.

The crystal structure of iGluR2 co-crystallized with the allosteric modulator cyclothiazide (CTZ, Scheme 1) provided the first structural evidence for the mechanism of positive allosteric modulation of the AMPA receptors [3]. The modulator was found to bind in the dimer interface between two iGluR2 subunits. The active receptor is known to be a tetrameric complex constituted of a dimer of dimers [4,5].

Allosteric modulators like CTZ exert at least part of their effect by inhibiting desensitization, which is the process of ion channel closure in the presence of an agonist [6]. As desensitization is thought to involve rearrangement of the dimer interface, it can be inhibited by the binding of a modulator in the interface resulting in increased ion channel open time [3,7]. This is in agreement with the observation that point mutations of residues located in the dimer interface observed in the crystal

* Corresponding author. Tel.: +45 35 30 65 05; fax: +45 35 30 60 40.

E-mail address: tl@dfuni.dk (T. Liljefors).

¹ Present address: Nuevolution A/S, Rønnegade 8, DK-2100 Copenhagen, Denmark.

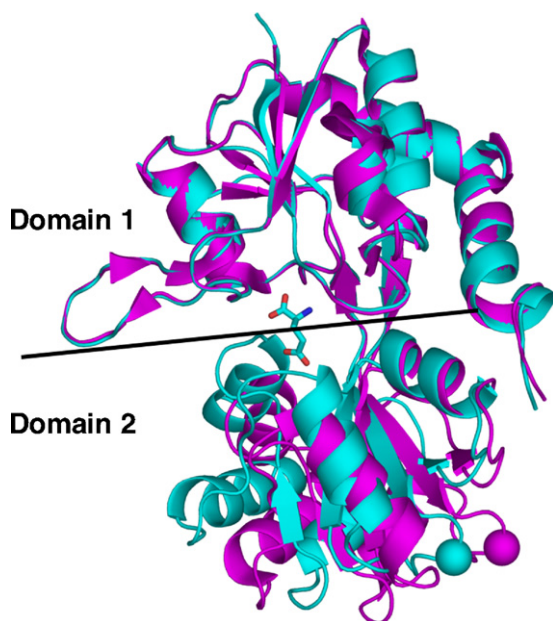
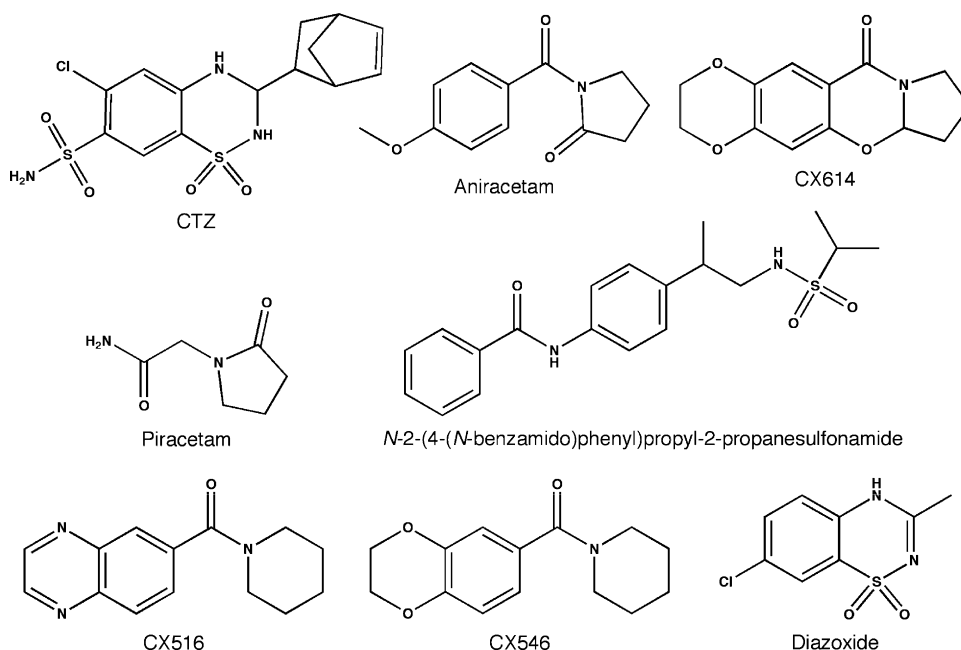


Fig. 1. Cartoon representation of the ligand binding domain of iGluR2 in complex with glutamate (cyan) and in the apo form (magenta). The proteins are superimposed by domain 1. The sphere marks the link to the ion channel in the full-length receptor and shows the movement induced by binding of glutamate (shown in stick representation in the center).

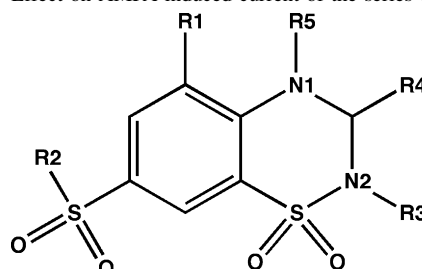
significantly alter desensitization and the regulation by positive allosteric modulators [3,8–11]. Furthermore, this strongly indicates that the dimer observed in the crystal structures is biologically relevant. In fact, Sun et al. [3] showed that the free-energy change for dimerization of the isolated LBDs of iGluR2 wildtype and mutants correlates with the free-energy change for desensitization observed for the full-length non-engineered receptor.

CTZ is only one of many compounds that have a positive effect on the currents mediated by AMPA receptors [12–15]. Two additional crystal structures of iGluR2 in complex with the allosteric modulators aniracetam and CX614 (Scheme 1), have recently been published [7]. The binding sites for these two modulators overlap with the binding site of CTZ. There are however strong indications that one or more additional binding sites for allosteric modulators, which do not overlap with the CTZ binding site, may exist. The results of a study by Fallarino et al. [16] show that radioactively labeled aniracetam could not be displaced by CTZ in concentrations up to 2 mM. Furthermore, high concentrations of CTZ increased the binding of aniracetam. This is in conflict with an exclusive binding of aniracetam to the binding site displayed in the crystal structure. However, the pharmacological data can be explained by the existence of a second binding site combined with an affinity of aniracetam for the two sites which depends on subtype and/or alternative subtype splice form (flip/flop) [11]. An allosteric effect of CTZ can then explain the observed increase in aniracetam binding. Zarrinmayeh et al. [13] used binding studies with another radioactively labeled modulator, *N*-2-(4-(*N*-benzamido)phenyl)propyl-2-propanesulfonamide (Scheme 1) to show that it is displaced by cyclothiazide but not by piracetam (Scheme 1). Another way to study competitive binding was employed by Arai et al. [15]. They utilized the effect of CTZ on agonist binding affinity to show that even high concentrations of the positive allosteric modulator, CX516 (Scheme 1) do not affect the dose-response relationship. They also showed that CX516 does not have an effect on the increase of agonist binding affinity of a very close analog, CX546 (Scheme 1). These results show that some modulators do not bind in the same site as CTZ or the overlapping sites of aniracetam and CX614. This indicates the presence of at least one additional binding site.



Scheme 1.

Table 1
Effect on AMPA induced current of the series of CTZ analogs



Compound	R1	R2	R3	R4	R5	% of control ^a
1	H	N(CH ₂ CH ₃) ₂	H	C ₆ H ₁₁	H	285
2	CH ₃	N(CH ₂ CH ₃) ₂	H	C ₆ H ₁₁	H	102
3	H	Morpholinyl	H	C ₆ H ₁₁	H	259
4	H	Morpholinyl	H	C ₆ H ₁₁	CH ₃	100
5	H	Morpholinyl	CH ₃	C ₆ H ₁₁	H	99
6	H	N(CH ₃) ₂	H	C ₆ H ₁₁	H	285
7	H	N(CH ₃) ₂	H	CH ₃	H	101

^a Potentiation of AMPA induced steady state current at a modulator concentration of 3 μ M, 100% corresponds to the control value.

In addition, different effects on receptor properties are observed for CTZ and analogs with the same core structure. The most active of the 5-alkyl-benzothiadiazide (5ABTD) allosteric modulators (compound 9, Table 2), enhances agonist

binding and *increases* the deactivation time constant 17-fold [17], whereas CTZ *decreases* agonist binding [18] and has a very limited effect on the deactivation time, only less than a 2-fold increase [19].

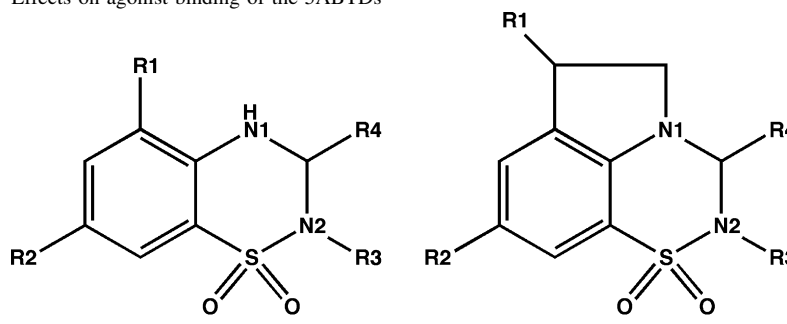
The aim of the present work is to show that the 5ABTDs reported by Phillips et al. [20] do not share binding site with CTZ despite their common core structure (Tables 1 and 2). This is done by comparing structure–activity relationship (SAR) data for this series of compounds [17,20] to previously unpublished SAR data for a series of very close analogs of CTZ in conjunction with the experimentally observed binding mode of CTZ. A new potential binding site in the dimer interface of GluR2 is identified and characterized. Docking studies are then used to show that the series of 5ABTDs can bind to this site and that the ligand–receptor interactions in the site are in agreement with SAR data for the 5ABTDs.

2. Methods

2.1. Pharmacology

The pharmacological data for compounds 1–7 (Table 1) were obtained by conventional whole cell patch clamp methods, essentially as previously described [21] using mouse neocortical neurons cultured as described by Drejer et al. [22].

Table 2
Effects on agonist binding of the 5ABTDs



Compound	R1	R2	R3	R4	EC ₅₀ (μ M) ^a
8 (IDRA21)	H	Cl	H	CH ₃	>500
9	CH ₂ CH ₃	Cl	H	CH ₃	17
10	CH ₂ CH ₃	H	H	CH ₃	101
11	CH(CH ₃) ₂	Cl	H	CH ₃	34
12	CH ₂ CH ₂ CH ₃	Cl	H	CH ₃	170
13	CH ₃	Cl	H	CH ₃	96
14	CH ₃	F	H	CH ₃	90
15	Cl	CH ₃	H	CH ₃	141
16	Cl	CH ₂ CH ₃	H	CH ₃	NE ^b
17	CH ₂ CH ₃	Cl	H	2 \times CH ₃ ^c	>400
18	CH ₃	F	H	H	127
19	CH ₃	F	H	CH ₂ CH ₃	178
20	CH ₃	F	H	C ₆ H ₅	NE ^d
21	CH ₂ CH ₃	Cl	(CH ₂) ₂ OH	CH ₃	69
22	H	Cl	H	CH ₃	85
23	CH ₃	Cl	H	CH ₃	18

^a Effect by the modulator on binding of a radioactively labeled agonist.

^b No effect at 120 μ M.

^c Geminal dimethyl substitution.

^d No effect at 200 μ M.

These data are measured as steady state current at a modulator concentration of 3 μM and given as percent of the control current induced by 30 μM AMPA.

2.2. Computational details

2.2.1. Proteins

The iGluR2 crystal structure coordinates used in this work were downloaded from the Protein Data Bank (PDB) [23]. The following ligand–protein complexes have been used (pdb codes within parentheses): glutamate/iGluR2 (1FTJ) [2], AMPA/iGluR2 (1FTM) [2], kainate/iGluR2 (1FW0) [2], cyclothiazide + glutamate/iGluR2 (1LBC) [3], quisqualate/iGluR2 (1MM7) [24], and 2-Me-Tet-AMPA/iGluR2 (1M5B) [25]. In addition, the apoform of iGluR2 (1FTO) [2] have been used.

A dimer of 1FW0 was created in Pymol [26] using the “symexp” command. For 1FTJ, 1FTM, 1LBC and 1M5B the dimer of chains A and C were used. Two dimers of 1MM7 were employed. The dimer of chains A and C were used for superimposition. For docking studies and for calculations of molecular interaction fields a dimer was created from chain B as described for 1FW0 with the new chain named D. The reason for using chains B and D for docking and GRID calculations is that chain B is the only chain in 1MM7 in which all amino acid residues in the dimer interface are fully resolved. A N754S mutant of the BD dimer was created using the mutate function in Maestro [27]. MolProbity [28] was used to check all dimers for errors with respect to histidine tautomeric form and erroneous side chain conformations of glutamines and asparagines. Suggested corrections were all accepted.

2.2.2. Cavity search in the iGluR2 LBD dimer

The PASS (putative active sites with spheres) program [29] was employed to characterize regions of buried volumes in 1FTJ and 1MM7 and to identify possible binding sites. The “allprobes” option was used to write all probes to the output file.

The residues comprising the identified cavity located in 1FTJ were superimposed onto the same residues of 1FTM, 1FTO, 1LBC, 1MM7 and 1M5B in Maestro [27] with “superimpose by ASL” using all atoms of the residues. In cases where the structures differ due to missing atoms or to mutations, only the atoms in question were omitted from the ASL expression.

2.2.3. Conformational analysis of 5ABTDs

Possible conformers for the core structure of the 5ABTDs were built in Maestro [27] and energy minimized using Gaussian03 [30] employing the B3LYP method, the 6-31G** basis set and the IEFPCM hydration model. For calculations of conformational energy penalties for binding for the core structures, a single point energy calculation was performed for gas phase with tight convergence using the same method and basis set. Estimates of conformational energy penalties for ligand binding with respect to substituent conformations were calculated by performing a 360° dihedral drive about the bond connecting the substituent to the aromatic ring with a step size of 2°. This was performed by using the MacroModel program [31] with the MMFFs force field and the TNCG minimization

method. The calculations were performed without a cutoff distance for non-bonded interactions and with water as solvent.

2.2.4. Calculations of molecular interaction fields

The GRID program [32,33] was used to determine energetically favorable binding sites for ligand binding in the 1MM7 dimer (chains B and D, see Section 2.2.1). In general, the grid dimensions in Å were set to TOPX/BOTX, 60/44; TOPY/BOTY, 76/60; TOPZ/BOTZ, 61/45 and the grid spacing (NPLA) was set to 3. The following probes were used: C3, N1, O, OH2. When GRID was used to position water molecules, NPLA was set to 5 and the utility programs in GRID, Minim and Filmap were employed using a threshold of –2 kcal/mol and interpolation. Water molecules not mediating hydrogen bonds between the protein and the modulator were deleted. When the binding site included **21**, the grid dimensions were set to TOPX/BOTX, 62/46; TOPY/BOTY, 80/64; TOPZ/BOTZ, 61/45. The k2f utility was used to convert the output contour files to a format readable by Pymol [26].

2.2.5. Docking and refinement

All dockings and refinements were performed using the program Glide [34–37]. Bond orders and atom types for the agonists and CTZ in 1LBC and 1MM7 were corrected in Maestro, all other HETATM records in the pdb file were deleted and hydrogen atoms were added. The first step of refinement in the protein preparation utility was performed to correct positions of polar hydrogen atoms of flexible moieties.

CTZ was then deleted from 1LBC and a grid was prepared with the center defined by residues Pro 494 and Ser 497 from both dimer chains. All three midpoint box diameters under “Advanced settings” were set to 14 Å and the “Dock ligands with length” was set to 10 Å. The docking was performed without scaling and default values were used for all other settings. Comparison of the output pose from Glide and the experimentally observed pose of CTZ was performed in Maestro by superimposition of all heavy atoms in common.

All Glide grids of 1MM7 were prepared with the center of the site defined by Phe 658 of chain B and Glu 755 of chain D and with all box settings at 8 Å. Dockings of CTZ, aniracetam, CX614, **9** and **21** were performed with a scaling of 0.7 (note that the default in Glide is 0.8 for regular docking and 0.5 for induced fit docking) for atoms with a partial atomic charge less than 0.9 and the output was set to a maximum of 10 poses per ligand. Simulation of induced fit was performed by running all steps of refinement in the protein preparation utility with the modulator and the tightly bound water molecules in the site. The ensuing dockings were performed as before but with the scaling changed to 0.9. Output poses were exported as pdb files and imported into Pymol [26] for comparison with the interaction energy contours from the GRID calculations (see Section 2.2.4).

2.2.6. Molecular electrostatic potentials

Structures were built in Maestro as described in Section 2.2.3 and imported into SPARTAN '02 [38]. To calculate molecular electrostatic potentials, a single point calculation

was performed using the Hartree–Fock model and the 6-31G** basis set.

3. Results and discussion

3.1. Comparison of SAR data for the CTZ analogs (1–7) and the 5ABTDs (8–23)

The SAR data used for the comparison are given in [Tables 1 and 2](#). The pharmacological effects of compounds **1–7** ([Table 1](#)) are based on observed potentiation of AMPA-induced steady state current, whereas the effects of the 5ABTDs, **8–23** ([Table 2](#)) are based on increase of agonist binding in the presence of the modulators [17,20]. However, the EC₅₀ for **8** and **9** with respect to increase of glutamate-induced currents is >400 μ M [39] and 36 μ M [17], respectively. These values are similar to those observed for the effect on agonist binding, EC₅₀ > 500 and 17 μ M for **8** and **9**, respectively ([Table 2](#)). Therefore, an approximate correlation between the effect on agonist binding and potentiation of agonist-induced current may be assumed. Based on this, a qualitative comparison of the SAR data of the two series of compounds may be performed.

The most important differences in the SAR data are summarized in [Table 3](#). In the 5ABTD series, small R1 alkyl substituents greatly enhance the activity. As shown in [Table 1](#), a methyl group decreases the EC₅₀ from >500 μ M (**8**) to 96 μ M (**13**). The opposite is observed for a R1 methyl substituent in the CTZ-analogs with a decrease in potentiation from 285% for **1** to the control level for **2** ([Table 1](#)). The same is observed for R3 and R5/N1 substitution. In the 5ABTD series, the EC₅₀ values for compounds **21** and **23** in comparison with that for compound **9** show that small alkyl substituents are tolerated in these positions with conservation of activity, indicating that there is room in the receptor for R3 and R5/N1 substituents. In contrast, a loss of potentiation is observed for the CTZ-analogs with R3 = methyl (**5**) and R5 = methyl (**4**) compared to the potentiation of the R3 and R5 unsubstituted compound **3**. The largest R2-substituent tested for the 5ABTDs is an ethyl group (**16**), which results in loss of activity ([Table 2](#)). However, all the CTZ-analogs ([Table 1](#)), active as well as inactive, have a R2 substituent including the sulfone moiety, which is considerably more bulky than an ethyl group. The last major difference is observed for the R4 substituent. For the 5ABTD series there is very little tolerance for R4-substitution and a methyl group is the optimal substituent (compare **14**, **19** and **20**). In contrast, replacing the R4 cyclohexyl group in **6** by a methyl group to

give **7** results in a complete loss of activity indicating that a bulky substituent is necessary for high activity in this series. Other studies also show that the substituent of CTZ corresponding to R4 has a large effect on the activity [40,41]. Removing the norbornenyl substituent in CTZ leads to an essentially inactive compound [39].

The significant differences in SAR data for the 5ABTDs and the CTZ-analogs summarized above and in [Table 3](#), strongly indicate that these two series of compounds cannot have the same binding site or binding mode in the AMPA receptors.

3.2. Comparisons to the observed binding mode of CTZ

The molecular structure of the active CTZ-analogs is similar to the structure of CTZ ([Scheme 1](#) and [Table 1](#)) and it may be assumed that they interact with the AMPA receptor in the same way. This implies that a different binding mode and maybe a different binding site exist for the 5ABTDs.

To validate this hypothesis, compounds **1–7** and the most active 5ABTD (**9**) were docked into the observed binding area of CTZ in iGluR2 by using the docking program Glide. To evaluate Glide, CTZ itself was included in the docking. The RMSD of the highest ranking output pose of CTZ compared to its binding pose in the crystal structure was found to be 0.19 Å proving that Glide is able to accurately dock this type of compounds. As assumed, **1**, **3** and **6** displayed a binding pose very similar to that of CTZ and the highest RMSD of all atoms in common with CTZ was calculated to be 0.44 Å. However, none of the output poses of the 5ABTD compound **9** were found to resemble the binding mode of CTZ and none of the top ranking poses displayed a reasonable hydrogen-bonding pattern to the receptor, nor are they able to explain the SAR data in [Table 2](#). These results confirm that the CTZ-analogs bind to the protein similar to CTZ and indicate that the binding site of the 5ABTDs has to be found elsewhere in the iGluR2 receptor.

3.3. Locating a putative binding site for the 5ABTDs

In the search for a potential binding site for the 5ABTDs, the program PASS [29] was used to detect cavities in the crystal structure of the iGluR2 ligand-binding domain including glutamate as bound agonist (the 1FTJ dimer, see [Section 2.2.1](#)). PASS fills cavities of the protein with probe spheres and assigns a burial count (BC) to each of them according to the number of protein atoms in its vicinity. The transparent grey surface in [Fig. 2](#) shows the surface of the PASS probes with BC \geq 70 and

Table 3
Summary of the differences in structure–activity relationships (SAR) for the CTZ-analogs (**1–7**) and the 5ABTDs (**2–23**)

	SAR for compounds 1–7	SAR for compounds 8–23
R1	Substitution results in loss of activity	Small alkyl substituents greatly enhance activity
R2	All compounds contain a sulfonamide group	F, Cl and methyl substituents give the best effect. Ethyl substitution is not tolerated
R3	Substitution results in loss of activity	Small hydrophilic substituents give the best effect
R4	A cyclohexyl group gives best effect. A methyl substituent leads to loss of activity	Very low tolerance for substitution. Methyl substitution gives best effect
R5/N1	Substitution results in a loss of activity	Small alkyl groups tolerated (22 and 23)

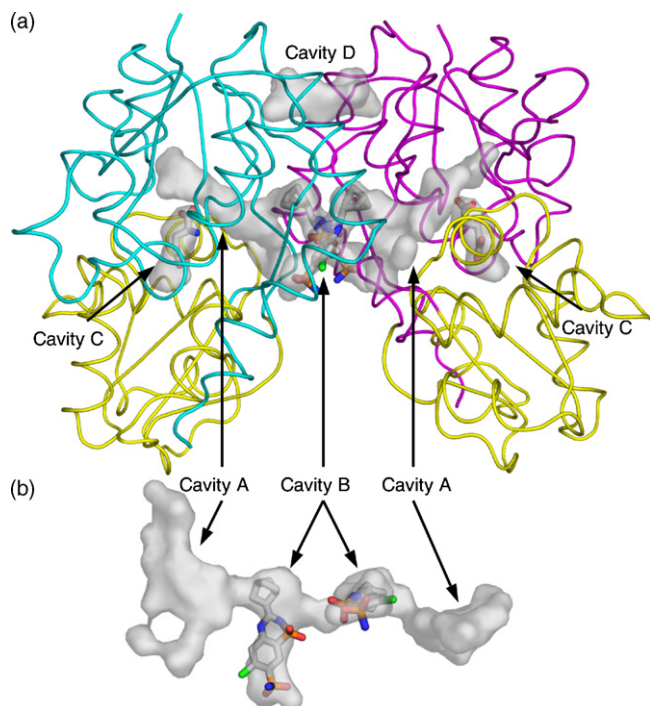


Fig. 2. In addition to the binding sites of glutamate (cavities C) and CTZ (cavities B), two symmetrically identical cavities (cavities A) and a cavity (cavity D) at the top of the dimer interface were identified by PASS for the dimer of the iGluR2 ligand binding domain. Domain 1 of chain A is cyan, domain 1 of chain C is magenta and domain 2 of both chains is yellow. (a) Surface of the PASS output probes with a $BC \geq 70$ for glutamate/iGluR2 (1FTJ) and (b) surfaces of cavities A and B superimposed onto CTZ.

clearly identifies the binding sites of the allosteric modulator CTZ (cavities B) and the agonist glutamate (cavities C). In addition, a cavity (cavity D) is located at the top of the dimer interface (Fig. 2a) adjacent to residue 743 which is subject to RNA editing from arginine to glycine in some receptor subtypes [42]. This cavity most probably contains the side chains of the arginines when the protein is unedited [2], indicating that the shape and size of this cavity will change with the editing level. IDRA21 (**8**) has a modulatory effect on both iGluR1 and iGluR2 receptors [43] even though iGluR1 is 100% unedited and iGluR2 is 80–90% edited [44]. Thus, it is unlikely that the 5ABTD modulators can bind in this cavity. Finally, a pair of cavities (cavities A) is located in the dimer interface adjacent to the binding site of CTZ (Fig. 2). Cavity A has a size that can accommodate the 5ABTDs and may thus be a binding cavity for these modulators. Due to the two-fold symmetry just one cavity A is further characterized and used for docking studies.

3.4. Characterization of cavity A

Residues 482–484, 654, 657–658, 661–662, 728 and 730 from one monomer and 754–755 from the other monomer define cavity A. The numbering corresponds to the full-length receptor excluding the signal peptide, i.e. the same numbering as that used by Armstrong and Gouaux [2]. To show that this cavity is a structurally conserved part of the dimer interface, the

crystal structures of iGluR2 in complex with the agonists glutamate [2], AMPA [2], glutamate plus CTZ [3], quisqualate [24] and 2-Met-Tet-AMPA [25] were superimposed (see Section 2.2.2). RMSDs between 0.47 and 0.78 Å were calculated showing that cavity A is structurally conserved when a full agonist is bound. On the other hand, if the structure with glutamate is compared to iGluR2 in the apo form [2] the RMSD increases to 4.77 Å. Residues 654, 657, 658 and 661–662 are located in domain 2 of the LBD (Fig. 1) and there is a difference of 20° in domain closure between the structure including a full agonist and the apo form [2]. Therefore, the positions of the residues in domain 2 change relative to domain 1 with the degree of domain closure. The iGluR2 structure to be used for further characterization of the cavity and docking studies must thus contain a full agonist to ensure that the cavity is structurally intact. The structure should be resolved to a good resolution (below 2.0 Å) and all residues of the cavity should be resolved. Based on this, chain B of the iGluR2-quisqualate structure (1MM7) [24] was selected. The dimer of this monomer, which corresponds to that of chains A and C used for the superimpositions, was created using the symmetry information in the pdb file as described in Section 2.2.1. A PASS analysis was performed on the selected protein to obtain a surface of all probes in cavity A.

To further characterize cavity A, the protein was stripped of water molecules and molecular interaction fields were calculated using the program GRID [32,33]. The methyl probe (C3) was used to calculate energetically favorable sites for lipophilic interactions. The planar amide nitrogen (N1) and the carbonyl oxygen (O) probes were used to locate favorable positions for hydrogen bond donor and acceptor groups, respectively. Furthermore, the water probe (OH2) was employed to locate positions of tightly bound water molecules. The calculated interaction energy contours from the GRID calculations and the PASS surface were used to evaluate ligand docking poses and to analyze the SAR data in Table 2.

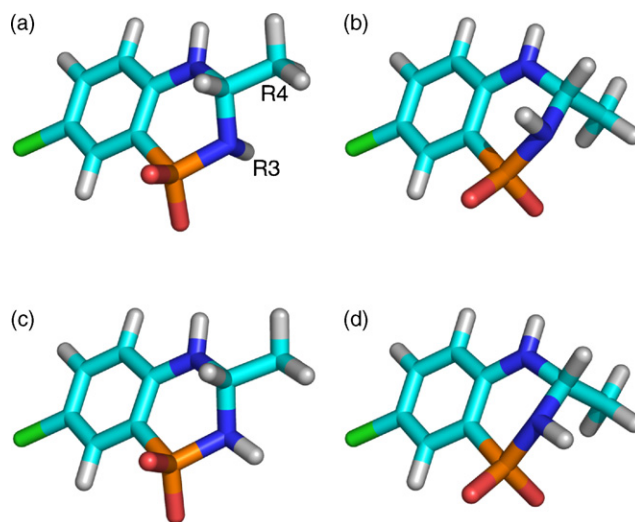


Fig. 3. The four possible conformers of **8** with *S*-configuration at the R4-substituent and the corresponding calculated conformational energies. (a) Global energy minimum; (b) +3.1 kcal/mol; (c) +3.6 kcal/mol; (d) +6.7 kcal/mol.

3.5. Conformational analysis of the 5ABTD core structure

Since the Glide docking program does not sample conformers of rigid ring structures as the 5ABTD core structure, a conformational analysis is necessary to identify possible bioactive conformations to be used as input structures. The only flexibility of the 5ABTD core resides in the sulfonamide ring. Two ring conformations are possible and the R3-substituent can be located in an axial or an equatorial position. Combined with the unspecified stereochemistry at the R4-substituent, there are four pairs of enantiomers. The four possible *S*-configuration conformations for **8** are displayed in Fig. 3.

An approach similar to the one described by Boström et al. [45] was employed to estimate conformational energy penalties for binding using a quantum chemical (QC) approach instead of force field calculations to increase the accuracy of the energy calculations. The gas phase conformational energy for each possible binding conformation was compared to the gas phase conformational energy of the global minimum conformation identified by a conformational analysis for aqueous phase. This was done by minimizing the four possible conformers of **8** using a solvation model and then calculating the conformational energy in vacuum. B3LYP/6-31G** was used for both calculations. The global energy minimum conformer (Fig. 3a) was found to have the R3 hydrogen atom in an axial position and the R4-substituent in an equatorial position. An axial R3

hydrogen position is also observed in small molecule crystal structures of compounds with the same core structure [46,47]. It is also indicated for CTZ in the 1LBC structure where the backbone carbonyl of Pro 494 is positioned 2.85 Å in an axial direction from the corresponding nitrogen in CTZ [3]. An equatorial position for the R3 hydrogen atom increases the conformational energy by 3.6 kcal/mol (Fig. 3c) and an axial position of R4 increases the energy by 3.1 kcal/mol (Fig. 3b). Boström et al. suggest a threshold of ca. 3 kcal/mol for the bioactive conformation for high-affinity compounds compared to the global energy minimum [45]. Because of the high conformational energy of the conformation in Fig. 3d, it is excluded as a potential binding conformation.

R3-substitution may have an impact on the conformation and therefore a similar conformational analysis was conducted with R3 = methyl. Results similar to those presented for **8** in Fig. 3 were obtained. Only the highest energy conformation, corresponding to that in Fig. 3d, was thus excluded as a possible binding conformation.

3.6. Finding a binding mode in cavity A for the 5ABTDs via docking with Glide

In order to find a reasonable binding mode in cavity A (Fig. 2) for the 5ABTDs by use of docking, it should be kept in mind that the cavity of the crystal structure does not contain a

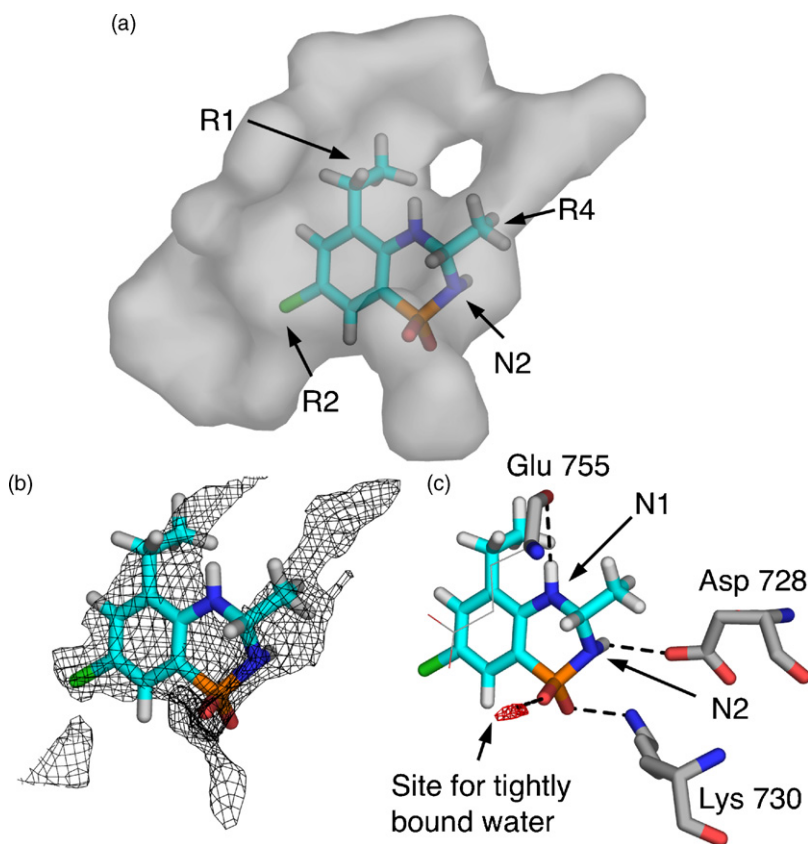


Fig. 4. The binding mode of **9** from docking into the putative binding site for the 5ABTDs. (a) Superimposed on the PASS surface. (b) Superimposed on the GRID interaction energy contour of a methyl probe at -3 kcal/mol. (c) Displayed with hydrogen bonds to the receptor (dashed lines) and a site for a tightly bound water molecule at -12 kcal/mol (red grid).

ligand. Thus, the protein may not be in an optimal conformation for binding of the 5ABTDs. In the docking program Glide [34–37] scaling the van der Waals radii of the modulator can be used to simulate a small degree of “induced fit”.

The ligand used to find the binding mode should be highly active in order to expect a good fit to the receptor. Compound **9** (Table 2), the most active of the 5ABTDs, was therefore used. The three lowest energy conformers (Fig. 3a–c) and their corresponding enantiomers were docked into cavity A with the van der Waals radius of all modulator atoms scaled by 0.7.

In the process of identifying the binding mode among the output poses from Glide, the fit of the pose to the GRID molecular interaction fields and the conformational energy of the poses were considered. Furthermore, the number of hydrogen bond possibilities that are fulfilled are important as unpaired hydrogen bond donor/acceptor atoms result in reduced binding affinity due to uncompensated energy cost of desolvation. The best pose, which is the lowest energy conformer of **9** with respect to the core structure, is shown in Fig. 4. The PASS surface represents the overall shape of the cavity and fully encloses the modulator **9** (Fig. 4a) showing that there are no steric clashes to the receptor. The methyl probe energy contour at -3 kcal/mol, which represents favorable van der Waals interactions with the protein, encloses almost the entire structure of **9** (Fig. 4b). An optimal dihedral of 76.5° for the bond between the R1 ethyl group and the aromatic ring is calculated by QC minimization of **9**. The dihedral of the selected pose is 76.6° indicating that there is no conformational penalty of binding. Furthermore, each hydrogen bond donor and acceptor in the modulator is in the vicinity of a hydrogen bond partner (Fig. 4c). N2 and one of the sulfonamide oxygens are within hydrogen bonding distance of the charged atoms of Asp 728 and Lys 730, respectively. This is confirmed by GRID calculations, which show that N2 is located at an energy level of -7 kcal/mol for the planar amine probe and the sulfonamide oxygen at -6.5 kcal/mol for the carbonyl probe. Within 3 Å of the other sulfonamide oxygen a position for a tightly bound water molecule with an interaction energy level of -12 kcal/mol was calculated (Fig. 4c). Furthermore, the selected pose does not overlap with any tightly bound water molecules, which

would otherwise disfavor binding. N1 is located 3.62 Å from the backbone carbonyl of Glu 755. The distance indicates a weak hydrogen bond, but it still represents a favorable interaction as N1 is positioned at an energy level of -7 kcal/mol for a hydrogen bond donor.

The importance of a hydrogen bond between N2 and Asp 728 is confirmed by comparing the pharmacological effects of **8** and diazoxide (Scheme 1). In diazoxide, the sulfonamide ring is planar and N2 is no longer a hydrogen bond donor. Bertolino et al. [39] show that, at a fixed concentration of 1 mM, **8** is four-fold more efficacious than diazoxide in potentiating glutamate responses. The hydrogen atom on N2 in the docking output poses of compound **9** with the *R*-configuration at R4 points away from Asp 728 making a hydrogen bond impossible. Thus, it may be predicted that the *S*-enantiomer is the most active enantiomer. If the pure enantiomers can be prepared they should display a marked difference in potency and activity.

CTZ, aniracetam and CX614 were also docked into cavity A and as expected the size and rigidity of CTZ and CX614 prevents them from fitting into the binding site. The output poses from Glide are located at the edge of cavity A protruding out of the site. On the contrary, aniracetam does display a reasonable binding pose, which can explain the conflicting data reported for this modulator (see Section 1). However, SAR data for aniracetam are not available to validate this pose.

3.7. Simulating an induced fit between the 5ABTDs and the receptor

In order to use cavity A and the binding mode identified to explain the SAR data of the 5ABTDs, it is important that the contacts to the receptor are as accurate as possible. As described above, the GRID program was used to find the position of a hydrogen bond mediating water molecule with respect to the modulator and the receptor (Fig. 4c). This water molecule was included in the receptor and an induced fit between the modulator and the receptor was simulated to relieve steric clashes and optimize hydrogen bonds. This was accomplished by running all five steps of the protein refinement utility in Glide corresponding to a RMSD of 0.5 Å measured on

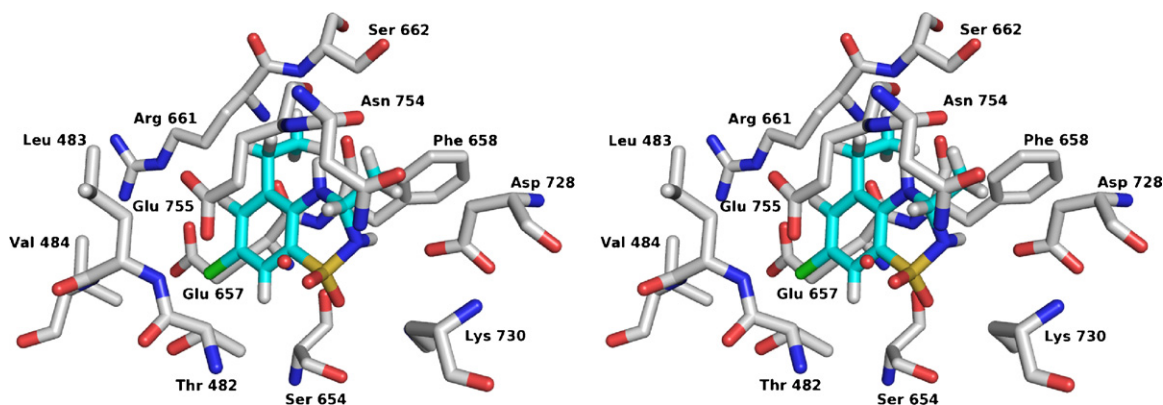


Fig. 5. Stereo image of the docked pose of compound **9** (cyan carbon atoms) in cavity A after simulation of induced fit. The included water molecule is shown as a red sphere.

all heavy atoms. This deviation is well within the RMSDs of the binding site observed between the crystal structures compared in Section 3.3 and only minor changes of the cavity are observed.

The “refined” protein was used to calculate new molecular interaction fields and to dock compounds **8–23** in order to find binding poses that can be used to give a detailed analysis of the SAR data. As the protein has been partly relaxed with respect to the most active modulator, a large scaling of the van der Waals radii was no longer necessary and it was thus set to 0.9. A stereo image of the binding site with compound **9** docked into it is shown in Fig. 5.

3.8. Validation of the proposed binding site

In order to make it probable that the 5ABTDs bind in cavity A, the binding mode suggested should be able to explain the SAR data in Table 2. In the following, the pharmacological data with respect to variations of R1–R4 and N1 substitution will be discussed in the light of calculated interactions between the 5ABTDs and the receptor.

3.8.1. R1-substitution

The most pronounced substituent effect in the series of 5ABTDs is observed for the R1-substituent. Replacing the hydrogen atom in **8** by a methyl (**13**) or an ethyl (**9**) group decreases the EC_{50} of the modulators from >500 to 96 and 17 μ M, respectively. Arai et al. [17] conclude that a major part of the surface of the ethyl substituent of **9** should be in contact with the receptor. This is in accordance with the binding mode proposed in this study. As illustrated in Fig. 6a, there is an unfilled pocket near the R1 hydrogen of **8** when it is docked into the proposed binding site. With **13** in the binding site, the methyl substituent protrudes into this pocket (Fig. 6b) but an ethyl group (**9**) is needed to completely fill it and gain optimal van der Waals interactions with the protein (Fig. 6c). If the size of the R1-substituent is increased to an isopropyl (**11**) or a propyl group (**12**) these substituents are still accommodated by the binding site represented by the PASS-surface (Fig. 6d and f). However, the energy contour of the methyl probe at -3 kcal/mol can no longer accommodate the entire substituents (Fig. 6e and g), which indicates that there is no additional gain in binding energy. The dihedral between the isopropyl and the

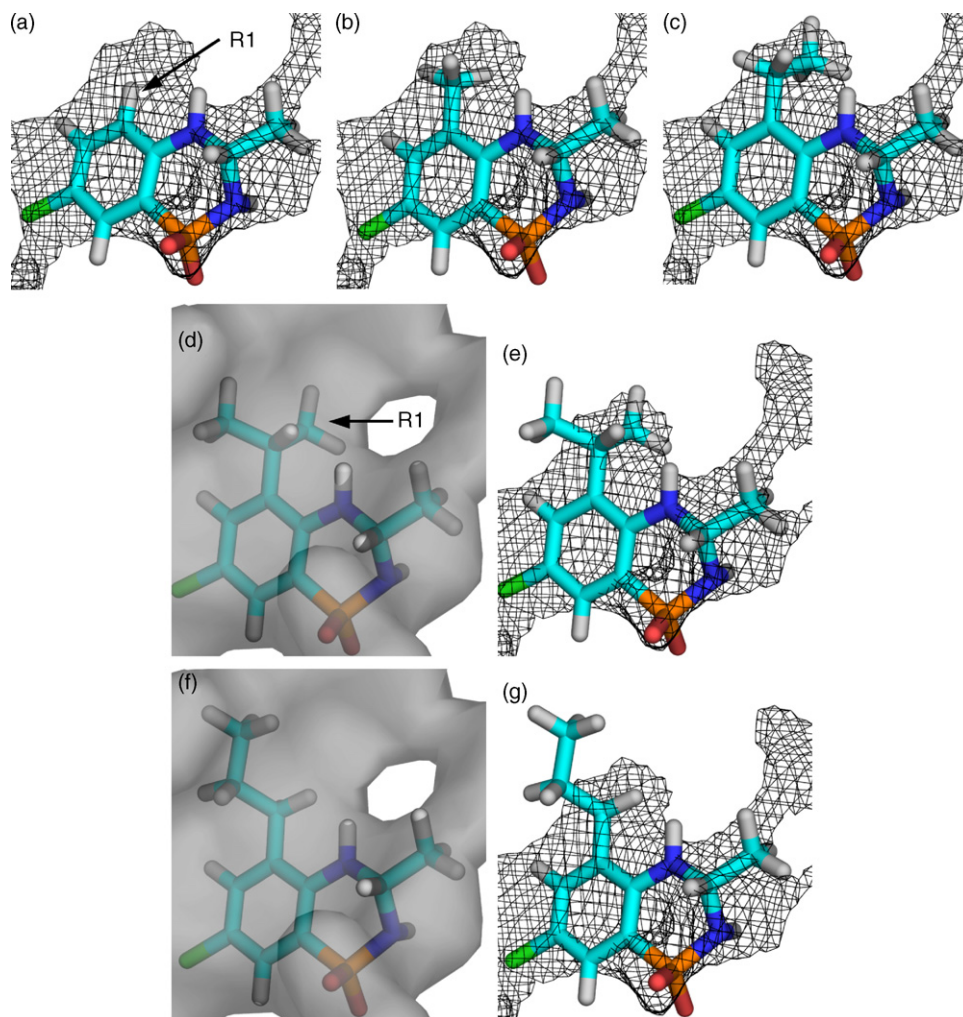


Fig. 6. Docking output poses for (a) **8**, (b) **13** and (c) **9** superimposed on the GRID interaction energy contour of a methyl probe at -3 kcal/mol. Docking output poses of (d and e) **11** and (f and g) **12** superimposed on the PASS surface (left) and the GRID interaction energy contour of a methyl probe at -3 kcal/mol (right).

aromatic ring of **11** only deviates by 7° from the minimum energy conformation indicating a low conformational penalty. Consequently, the EC_{50} of **11** is expected to be similar to that of **9**, which is also observed (Table 2). In the case of **12**, the very favorable interaction of the ethyl group in **9** is lost, as the propyl group finds another orientation in order to fit in cavity A (Fig. 6g). Furthermore, a conformational energy penalty of the binding conformation of **12** is estimated by molecular mechanics calculations to be ca. 2 kcal/mol. Such an energy penalty will result in a marked reduction in binding affinity [48] which corresponds to the observed 10-fold increase in the EC_{50} value for **12** compared to that of **9** (Table 2).

The EC_{50} values in Table 2 show that the R1-substituent has a strong effect on agonist binding. The dockings of **9** and **11–13** show that R1 have van der Waals contacts to residues Glu 657, Phe 658 and Arg 661, which are part of domain 2 and which moves in the process of agonist binding (Fig. 1). The interactions between these residues and the R1-substituent will thus stabilize the closed binding domain. This is expected to increase the rate of LBD closure as well as decrease the rate of LBD opening. This will in both cases result in an increased agonist binding affinity. Furthermore, as the properties of the binding site itself depend on the domain closure, the presence of an agonist should also increase the binding of the modulator. In fact, Arai et al. [17] state that EC_{50} values from measurements with short-term glutamate application were higher than with long-term applications suggesting that the modulator and agonist mutually increase the affinity of each other.

Additionally, Arai et al. show an increase of the deactivation time constant with increasing size of the R1-substituent [17]. Deactivation is the process of unbinding of the agonist and it has also been suggested to be related to the stabilizing effect on the closed LBD [7]. Studies have shown that CTZ on the contrary has a negative effect on agonist binding [15,18,40] and nearly no effect on deactivation [19].

This corresponds to the fact that the CTZ binding site is made up by residues almost exclusively from domain 1 [3].

The R1-substituent also has an effect on the ability of the compounds to affect desensitization. At a concentration of 200 μ M, **13** and **9** completely block desensitization, whereas **8** has only a slight potentiating effect [17]. In this regard, **9** and **13** have the same effect as CTZ. Common for the binding site of CTZ and the one identified in this study is that they are both located in the dimer interface (Fig. 2). Thus, as for CTZ, the 5ABTDs strengthen the interactions between the two monomers and prevent rearrangement of the dimer [3].

3.8.2. R2-substitution

The SAR data in Table 2 show that a R2-substituent with one heavy atom is optimal. A chloro substituent increases the potency significantly (**9** versus **10**). Furthermore, the results for **15** and **16** show a loss of potency when the substituent increases in size from a methyl to an ethyl group. Fig. 7a and b shows the two compounds superimposed on the energy contour of the methyl probe with the energy level set to -2 kcal/mol. The fact that the R2 methyl group of **15** is enclosed in the energy contour (Fig. 7a) shows that there is favorable interaction energy to gain by filling this part of the binding site. This explains the increased potency of **9** compared to **10**. The energy contour can also accommodate the ethyl group of **16** (Fig. 7b), which displays lower potency than **15** (Table 2). However, molecular mechanics calculations show that the dihedral angle of 25.4° displayed by the docking output pose involves a 1.1 kcal/mol conformational energy penalty. This corresponds to approximately a decrease by factor 10 in binding affinity [48].

3.8.3. R4-substitution

The R4-substituent is a methyl group in the most active of the 5ABTDs (compound **9**, $EC_{50} = 17 \mu$ M). If an additional methyl group is introduced in this position to give **17**, the result

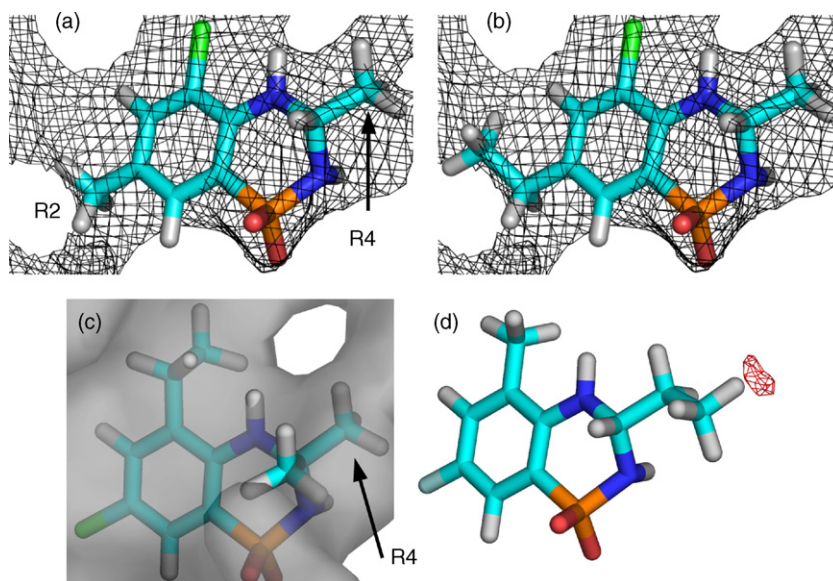


Fig. 7. Docking output poses of (a) **15** and (b) **16** superimposed on the GRID interaction energy contour of a methyl probe at -2 kcal/mol. Docking output poses of (c) **17** superimposed on the PASS surface and (d) **19** superimposed on the GRID interaction energy contour of a water probe at -13 kcal/mol.

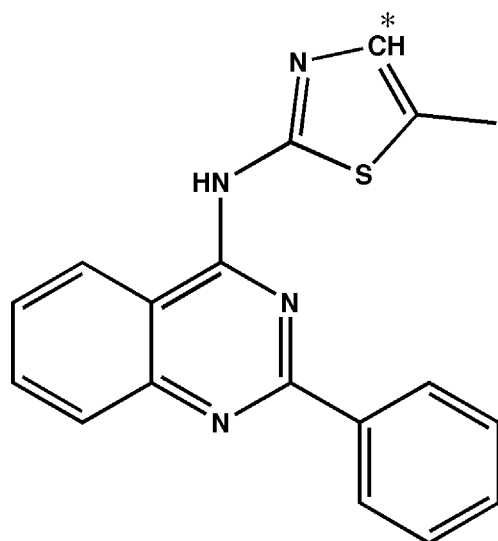
is a significant loss of potency, $EC_{50} > 400 \mu\text{M}$ (Table 2). As displayed in Fig. 7c, the axial methyl group of **17** protrudes out of the PASS surface of cavity A indicating a severe steric clash with the receptor which will markedly decrease the activity. If the potency of **14** is compared to those of **18** and **19** it is observed that a methyl group is the optimal R4 substituent although the variations in EC_{50} for a hydrogen (**18**), methyl (**14**) and an ethyl (**19**) substituent is within a factor of 2. This small difference in potency is in contrast to what that observed for the R1-substituent. However, the R4-substituent has very limited contacts to the residues of domain 2, which explains its minor effect on agonist binding.

The R4 methyl is enclosed in the energy contour of a methyl probe at -2 kcal/mol (Fig. 7a and b) and thus has favorable van der Waals interactions to the receptor. Removing this substituent to give **18** will, as observed, decrease the activity. In the case of **19**, the R4 ethyl group comes into steric conflict with a calculated position for a tightly bound water molecule (Fig. 7d), which affects the activity in a negative direction. At the same time, there is no interaction energy gain from the additional carbon atom, as it does not fit in a low energy conformation into the energy contour of the methyl probe at a favorable energy value. Increasing the size of the R4-substituent to a phenyl group (**20**) abolishes the activity at the tested concentration. According to the results, this is caused by a combination of steric clashes with the receptor, replacement of the water molecule and the conformational energy penalty of binding.

3.8.4. N1-substitution

The only structural difference between **13** and **22** and between **9** and **23** is a carbon atom, which connects N1 and the R1-substituent in **9** and **13** forming a 5-membered ring system. As shown in Table 2, this structural difference does not affect the EC_{50} values, which strongly indicates that the R1-substituents in these compounds should be located in the same pocket in the binding cavity. In order for this to be possible, the

additional stereogenic center of **23** must have an *S*-configuration. There should also be a positive interaction to the protein that compensates for the loss of the weak hydrogen bond between N1 in compounds **9** and **13** and the backbone carbonyl of Glu 755 (Fig. 4c). However, as seen in Fig. 4, N1 is located at the edge of the energy contour, indicating that substitution in this position will decrease the potency. It is however known that electrostatic interactions between carbonyl oxygens and hydrogen atoms of CH_2 -groups bonded to nitrogen atoms are present in small molecule crystal structures [49] and in protein–protein [50] and ligand–protein interactions [51]. Pierce et al. [52] show that an interaction referred to as a $\text{CH} \cdots \text{O}$ hydrogen bond is observed in a crystal structure. The ligand is shown in Scheme 2 and an asterisk marks the hydrogen atom involved in the hydrogen bond. In order to investigate if such a hydrogen bond is possible for compound **23**, molecular electrostatic potentials were calculated for **23** and for the molecule employed in the study by Pierce et al. and displayed in Scheme 2. The calculations were performed using the HF/6-31G** method and basis set. The maximum electrostatic potential on the surface of the hydrogen marked by an asterisk in Scheme 2 is calculated to be $+22.3 \text{ kcal/mol}$. The corresponding value calculated for the two hydrogen atoms of **23** is $+30.9$ and $+26.1 \text{ kcal/mol}$ for the equatorial and axial hydrogen, respectively. The more positive electrostatic potentials for **23** compared to those of the reference molecule indicates the feasibility of a $\text{CH} \cdots \text{O}$ hydrogen bond between **23** and Glu 755. The docking program Glide does not take $\text{CH} \cdots \text{O}$ hydrogen bonds into account and thus the docked poses cannot be expected to reflect ideal geometries for such interactions. However, the geometrical parameters with respect to the equatorial hydrogen in **23** (Fig. 8), which is closest to the Glu 755 carbonyl oxygen, match those obtained in a stereochemical analysis of $\text{C-H} \cdots \text{O}$ hydrogen bonds made by Derewenda et al. [50]. Thus, as shown in Fig. 8, compound **23** may have electrostatic interactions/hydrogen bonds to the same residues in the receptor as **9** does (compare with Fig. 4c).



Scheme 2.

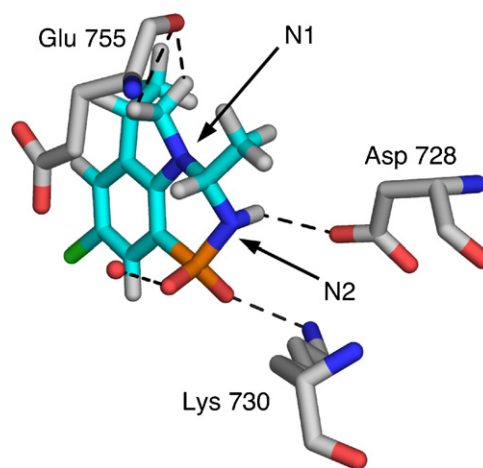


Fig. 8. Docking output pose of **23**. Hydrogen bonds and the electrostatic $\text{CH} \cdots \text{O}$ interactions to the receptor and a tightly bound water molecule (red sphere) are represented as dashed lines.

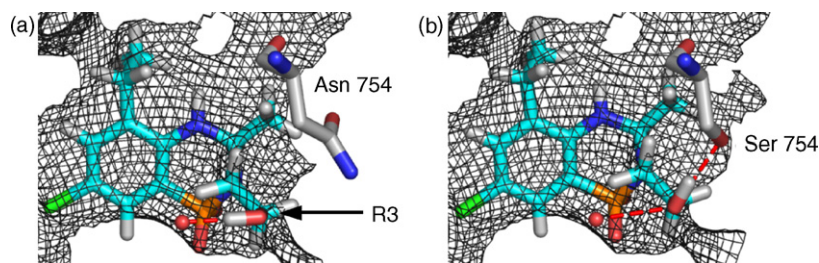


Fig. 9. Docking output poses of **21** in the binding cavity of (a) the flop splice form of iGluR2 and (b) a mutant resembling the flip splice form superimposed on the interaction energy contour of a methyl probe at -2 kcal/mol.

3.8.5. R3-substitution

Compound **21** is the most active R3 substituted compound of the 5ABTDs studied by Phillips et al. [20]. Since N2 for e.g. **9** has a hydrogen bond to Asp 728 (Fig. 4) there is no room in the cavity for a R3-substituent if the sulfonamide ring conformation is retained. Accordingly, the *S*-enantiomer of **21** does not dock properly into cavity A. However, the potency of **21** ($EC_{50} = 69 \mu\text{M}$, Table 2) indicates that R3-substitution is compatible with a significant activity and it was therefore investigated if **21** may bind to the receptor as its *R*-stereoisomer. If this is true, the R3-substituent will point towards Asn 754, which is subject to alternative splicing. Mutation of this asparagine (flop splice form) into a serine (flip splice form) has been shown to convert the behavior of AMPA receptors from flop to flip with respect to the pharmacological effect of other allosteric modulators [11]. Therefore, Asn 754 was replaced by serine and the procedure of identifying the binding mode described above was repeated with the *R*-stereoisomer of **21** in the original protein structure as well as in the mutated structure. The binding poses of *R*-**21** predicted by Glide dockings into cavity A of the two protein structures display a good fit to the methyl probe energy contour at -2 kcal/mol and only differ in the conformation of the hydroxy group (Fig. 9). They display the same position of the core structure as for the rest of the 5ABTDs but have a flip of the sulfonamide ring. However, the contacts of **21** to Asn 754 (Fig. 9a) and Ser 754 (Fig. 9b) are different. During the induced fit simulation the side chain of Asn 754 rotates from 33.1° to -29.5° about the CA-CB-CG-OD1 dihedral in order to compensate for a steric clash with the hydroxy group of **21** (Fig. 9a). This abolishes the possibility of a hydrogen bond between Asn 754 and **21**. In contrast, Ser 754 of the mutant is in a perfect position to make a strong hydrogen bond to the R3-substituent of **21** (Fig. 9b). This is similar to what is observed for CTZ [3], which displays a marked preferences for the flip splice form of the AMPA receptors [11]. Therefore, a preference for the flip-form over the flop-form for compound **21** is predicted. The work by Arai et al. [17] describes a flip preference with a selectivity ratio of 1.6 for **9** at iGluR2 receptors. This very weak selectivity indicates that there is no direct contact to residue 754, which is in agreement with the binding mode proposed in the present work for 5ABTDs that do not contain R3-substituents. The flip/flop selectivity for compound **21** or similar compounds has not been reported.

With **21** present in the binding site, GRID calculations identified a position for a tightly bound water molecule (-15 kcal/mol) near the hydroxy group of R3 in both receptor

splice forms (Fig. 9). A hydrogen bond to this water molecule is also expected to be important for the potency of **21**. In fact, all the active compounds with R3-substituents reported by Phillips et al. have donor/acceptor functions on the β -carbon of R3 [20]. However, due to the fact that the R3-substituent affects the location of the water molecule, the hydrogen bond to the sulfonamide oxygen is lost. This is at least partly made up for by the interactions of the hydroxy group and the positive van der Waals interactions of the R3-substituent.

4. Conclusion

A new cavity of a size that can accommodate drug-like molecules has been identified in the binding domain of iGluR2. Its location in the dimer interface and the fact that residues of both domains 1 and 2 are involved offers a mechanistic explanation for the effect on desensitization, deactivation and agonist binding for compounds that bind here. SAR data for 5ABTD allosteric modulators and for a series of close analogs of cyclothiazide indicate that these two classes of modulators do not bind to the same binding site. Docking of a series of 5ABTD allosteric modulators into the new cavity indicates that it may be the binding site for this class of allosteric modulators. It is furthermore shown that the SAR data available for the 5ABTDs are in very good agreement with the calculated binding mode in this cavity. The docking output poses combined with GRID molecular interaction fields of different probes are able to rationalize essentially all substituent effects on the activity of the 5ABTD modulators.

References

- [1] E. Gouaux, Structure and function of AMPA receptors, *J. Physiol. (London)* 554 (2004) 249–253.
- [2] N. Armstrong, E. Gouaux, Mechanisms for activation and antagonism of an AMPA-sensitive glutamate receptor: crystal structures of the GluR2 ligand binding core, *Neuron* 28 (2000) 165–181.
- [3] Y. Sun, R. Olson, M. Horning, N. Armstrong, M. Mayer, E. Gouaux, Mechanism of glutamate receptor desensitization, *Nature* 417 (2002) 245–253.
- [4] W. Tichelaar, M. Saffierling, K. Keinänen, H. Stark, D.R. Madden, The three-dimensional structure of an ionotropic glutamate receptor reveals a dimer-of-dimers assembly, *J. Mol. Biol.* 344 (2004) 435–442.
- [5] S. Matsuda, Y. Kamiya, M. Yuzaki, Roles of the N-terminal domain on the function and quaternary structure of the ionotropic glutamate receptor, *J. Biol. Chem.* 280 (2005) 20021–20029.
- [6] M.V. Jones, G.L. Westbrook, The impact of receptor desensitization on fast synaptic transmission, *Trends Neurosci.* 19 (1996) 96–101.

- [7] R.S. Jin, S. Clark, A.M. Weeks, J.T. Dudman, E. Gouaux, K.M. Partin, Mechanism of positive allosteric modulators acting on AMPA receptors, *J. Neurosci.* 25 (2005) 9027–9036.
- [8] M.S. Horning, M.L. Mayer, Regulation of AMPA receptor gating by ligand binding core dimers, *Neuron* 41 (2004) 379–388.
- [9] Y. Stern-Bach, S. Russo, M. Neuman, C. Rosenmund, A point mutation in the glutamate binding site blocks desensitization of AMPA receptors, *Neuron* 21 (1998) 907–918.
- [10] J.D. Leever, S. Clark, A.M. Weeks, K.M. Partin, Identification of a site in GluR1 and GluR2 that is important for modulation of deactivation and desensitization, *Mol. Pharmacol.* 64 (2003) 5–10.
- [11] K.M. Partin, M.W. Fleck, M.L. Mayer, AMPA receptor flip/flop mutants affecting deactivation, desensitization, and modulation by cyclothiazide, aniracetam and thiocyanate, *J. Neurosci.* 16 (1996) 6634–6647.
- [12] T.A. Shepherd, J.A. Aikins, D. Bleakman, B.E. Cantrell, J.P. Rearick, R.L. Simon, E.C.R. Smith, G.A. Stephenson, D.M. Zimmerman, Design and synthesis of a novel series of 1,2-disubstituted cyclopentanes as small, potent potentiators of 2-amino-3-(3-hydroxy-5-methyl-isoxazol-4-yl)propanoic acid (AMPA) receptors, *J. Med. Chem.* 45 (2002) 2101–2111.
- [13] H. Zarrinmayeh, D. Bleakman, M.R. Gates, H. Yu, D.M. Zimmerman, P.L. Ornstein, T. McKennon, M.B. Arnold, W.J. Wheeler, P. Skolnick, [³H]N-2-(4-(N-benzamido)phenyl)propyl-2-propanesulfonamide: a novel AMPA receptor potentiator and radioligand, *J. Med. Chem.* 44 (2001) 302–304.
- [14] P.L. Ornstein, D.M. Zimmerman, M.B. Arnold, T.J. Bleisch, B. Cantrell, R. Simon, H. Zarrinmayeh, S.R. Baker, M. Gates, J.P. Tizzano, D. Bleakman, A. Mandelzys, K.R. Jarvie, K. Ho, M. Deverill, R.K. Kamboj, Biarylpropylsulfonamides as novel, potent potentiators of 2-amino-3-(5-methyl-3-hydroxyisoxazol-4-yl)-propanoic acid (AMPA) receptors, *J. Med. Chem.* 43 (2000) 4354–4358.
- [15] A.C. Arai, Y.F. Xia, G. Rogers, G. Lynch, M. Kessler, Benzamide-type AMPA receptor modulators form two subfamilies with distinct modes of action, *J. Pharmacol. Exp. Ther.* 303 (2002) 1075–1085.
- [16] F. Fallarino, A.A. Genazzani, S. Silla, M.R. L'Episcopo, O. Camici, L. Corazzi, F. Nicoletti, M.C. Fioretti, [³H]Aniracetam binds to specific recognition sites in brain membranes, *J. Neurochem.* 65 (1995) 912–918.
- [17] A.C. Arai, Y.F. Xia, M. Kessler, D. Phillips, R. Chamberlin, R. Granger, G. Lynch, Effects of 5'-alkyl-benzothiadiazides on (R,S)- α -amino-3-hydroxy-5-methyl-4-isoxazolepropionic acid (AMPA) receptor biophysics and synaptic responses, *Mol. Pharmacol.* 62 (2002) 566–577.
- [18] M. Kessler, A. Arai, A. Quan, G. Lynch, Effect of cyclothiazide on binding properties of AMPA-type glutamate receptors: lack of competition between cyclothiazide and GYKI 52466, *Mol. Pharmacol.* 49 (1996) 123–131.
- [19] A. Arai, G. Lynch, The waveform of synaptic transmission at hippocampal synapses is not determined by AMPA receptor desensitization, *Brain Res.* 799 (1998) 230–234.
- [20] D. Phillips, J. Sonnenberg, A.C. Arai, R. Vaswani, P.O. Krutzik, T. Kleisli, M. Kessler, R. Granger, G. Lynch, A.R. Chamberlin, 5'-Alkyl-benzothiadiazides: a new subgroup of AMPA receptor modulators with improved affinity, *Bioorg. Med. Chem.* 10 (2002) 1229–1248.
- [21] C. Mathiesen, T. Varming, L.H. Jensen, In vivo and in vitro evaluation of AMPA receptor antagonists in rat hippocampal neurones and cultured mouse cortical neurones, *Eur. J. Pharmacol.* 353 (1998) 159–167.
- [22] J. Drejer, T. Honoré, A. Schousboe, Excitatory amino acid-induced release of ³H-GABA from cultured mouse cerebral cortex interneurons, *J. Neurosci.* 7 (1987) 2910–2916.
- [23] H.M. Berman, J. Westbrook, Z. Feng, G. Gilliland, T.N. Bhat, H. Weissig, I.N. Shindyalov, P.E. Bourne, The Protein Data Bank, *Nucl. Acids Res.* 28 (2000) 235–242.
- [24] R.S. Jin, M. Horning, M.L. Mayer, E. Gouaux, Mechanism of activation and selectivity in a ligand-gated ion channel: structural and functional studies of GluR2 and quisqualate, *Biochemistry* 41 (2002) 15635–15643.
- [25] A. Hogner, J.S. Kastrop, R. Jin, T. Liljefors, M.L. Mayer, J. Egebjerg, I.K. Larsen, E. Gouaux, Structural basis for AMPA receptor activation and ligand selectivity: crystal structures of five agonist complexes with the GluR2 ligand-binding core, *J. Mol. Biol.* 322 (2002) 93–109.
- [26] The Pymol Molecular Graphics System, version 0.98, Delano Scientific, San Carlos, CA, 2002.
- [27] Maestro, version 7.5.106, Schrödinger, Inc., Portland, OR, 2006.
- [28] I.W. Davis, L.W. Murray, J.S. Richardson, D.C. Richardson, MolProbity: structure validation and all-atom contact analysis for nucleic acids and their complexes, *Nucl. Acids Res.* 32 (2004) W615–W619.
- [29] G.P. Brady, P.F.W. Stouten, Fast prediction and visualization of protein binding pockets with PASS, *J. Comput.-Aided Mol. Des.* 14 (2000) 383–401.
- [30] Gaussian 03, revision C.02, Gaussian, Inc., Wallingford, CT, 2004.
- [31] MacroModel, version 9.1.106, Schrödinger, Inc., Portland, OR, 2006.
- [32] GRID, version 22a, Molecular Discovery Ltd., Pinner, Middlesex, 2005.
- [33] P.J. Goodford, A computational procedure for determining energetically favorable binding sites on biologically important macromolecules, *J. Med. Chem.* 28 (1985) 849–857.
- [34] Glide, version 4.0.108, Schrödinger, Inc., Portland, OR, 2006.
- [35] R.A. Friesner, J.L. Banks, R.B. Murphy, T.A. Halgren, J.J. Klicic, D.T. Mainz, M.P. Repasky, E.H. Knoll, M. Shelley, J.K. Perry, D.E. Shaw, P. Francis, P.S. Shenkin, Glide: a new approach for rapid, accurate docking and scoring. 1. Method and assessment of docking accuracy, *J. Med. Chem.* 47 (2004) 1739–1749.
- [36] T.A. Halgren, R.B. Murphy, R.A. Friesner, H.S. Beard, L.L. Frye, W.T. Pollard, J.L. Banks, Glide: a new approach for rapid, accurate docking and scoring. 2. Enrichment factors in database screening, *J. Med. Chem.* 47 (2004) 1750–1759.
- [37] W. Sherman, T. Day, M.P. Jacobson, R.A. Friesner, R. Farid, Novel procedure for modeling ligand/receptor induced fit effects, *J. Med. Chem.* 49 (2006) 534–553.
- [38] SPARTAN '02, version 119a, Wavefunction, Inc., Irvine, CA, 2002.
- [39] M. Bertolino, M. Baraldi, C. Parenti, D. Braghieri, M. Dibella, S. Vicini, E. Costa, Modulation of AMPA/kainate receptors by analogs of diazoxide and cyclothiazide in thin slices of rat hippocampus, *Recept. Channels* 1 (1993) 267–278.
- [40] M. Kessler, G. Rogers, A. Arai, The norbornenyl moiety of cyclothiazide determines the preference for flip–flop variants of AMPA receptor subunits, *Neurosci. Lett.* 287 (2000) 161–165.
- [41] K.A. Yamada, C.M. Tang, Benzothiadiazides inhibit rapid glutamate receptor desensitization and enhance glutamatergic synaptic currents, *J. Neurosci.* 13 (1993) 3904–3915.
- [42] H. Lomeli, J. Mosbacher, T. Melcher, T. Hoyer, J.R.P. Geiger, T. Kuner, H. Monyer, M. Higuchi, A. Bach, P.H. Seeburg, Control of kinetic properties of AMPA receptor channels by nuclear RNA editing, *Science* 266 (1994) 1709–1713.
- [43] N. Nagarajan, C. Quast, A.R. Boxall, M. Shahid, C. Rosenmund, Mechanism and impact of allosteric AMPA receptor modulation by the Ampakine™ CX546, *Neuropharmacology* 41 (2001) 650–663.
- [44] S.S. Jayakar, M. Dikshit, AMPA receptor regulation mechanisms: future target for safer neuroprotective drugs, *Int. J. Neurosci.* 114 (2004) 695–734.
- [45] J. Boström, P.O. Norrby, T. Liljefors, Conformational energy penalties of protein-bound ligands, *J. Comput.-Aided Mol. Des.* 12 (1998) 383–396.
- [46] L. Dupont, O. Dideberg, Crystal structure of hydrochlorothiazide, C₇H₈ClN₃O₄S₂, *Acta Crystallogr. Sect. B* 28 (1972) 2340–2347.
- [47] A.K. Basak, M. Ghosh, S.K. Mazumdar, S. Chaudhuri, Crystal and molecular-structure of 6-chloro-3-cyclopentylmethyl-3,4-dihydro-7-sulfamyl-2H-1,2,4-benzothiadiazine-1,1-dioxide, *J. Cryst. Spectrosc. Res.* 19 (1989) 547–560.
- [48] T. Liljefors, I. Pettersson, Computer-aided development of three-dimensional pharmacophore models, in: P. Krosgaard-Larsen, T. Liljefors, U. Madsen (Eds.), *A Textbook of Drug Design and Development*, second ed., Overseas Publishers Association, Amsterdam, 1996, pp. 60–93.
- [49] R. Taylor, O. Kennard, Crystallographic evidence for the existence of C–H···O, C–H···N, and C–H···Cl hydrogen-bonds, *J. Am. Chem. Soc.* 104 (1982) 5063–5070.
- [50] Z.S. Derewenda, L. Lee, U. Derewenda, The occurrence of C–H···O hydrogen-bonds in proteins, *J. Mol. Biol.* 252 (1995) 248–262.
- [51] A.C. Pierce, K.L. Sandretto, G.W. Bemis, Kinase inhibitors and the case for CH···O hydrogen bonds in protein–ligand binding, *Proteins: Struct. Funct. Genet.* 49 (2002) 567–576.
- [52] A.C. Pierce, E. Ter Haar, H.M. Binch, D.P. Kay, S.R. Patel, P. Li, CH···O and CH···N hydrogen bonds in ligand design: a novel quinazolin-4-ylthiazol-2-ylamine protein kinase inhibitor, *J. Med. Chem.* 48 (2005) 1278–1281.